Utilisation of glass wool waste and mine tailings in high performance building ceramics

Patrick N. Lemougna[1*], Juho Yliniemi [1*], Hoang Nguyen[1], Elijah Adesanya[1], Pekka Tanskanen[2], Paivo Kinnunen[1], Juha Roning [3] and Mirja Illikainen[1]

[1]Faculty of Technology, Fibre and Particle Engineering Research Unit, PO Box 4300, 90014 University of Oulu, Finland.
[2]Process Metallurgy Research Unit, University of Oulu, P.O. Box 4300, 90014 Oulu, Finland.
[3]InfoTech Oulu, Faculty of Information Technology and Electrical Engineering, Biomimetics and Intelligent Systems Group (BISG), University of Oulu, Oulu, Finland

*Corresponding author: Patrick.LemougnaNinla@oulu.fi ; lemougna@yahoo.fr (PNL)

Juho.Yliniemi@oulu.fi (JY)

Abstract:

The generation of glass wool waste and mine tailings has raised increasing concerns. This paper deals with the reuse of glass wool waste and lithium mine tailings from spodumene ore (quartz feldspar sand; QFS) in the development of building ceramic materials. The effect of glass wool particle size and sintering temperatures (750, 850 and 950 °C) were investigated. Phase composition and sintering reactions were studied using several techniques including X-ray diffraction with Rietveld refinement, differential scanning calorimetry, scanning electron microscopy, density, water absorption and mechanical tests. The results showed that glass wool acted as fluxing agent, with melting reactions observed from about 700 °C. Grinding glass wool improved its reactivity, enhancing densification and strength development at lower temperatures. The properties of the prepared building ceramics satisfied the requirement of building materials according to ASTM C62, achieving high performance values of 90 MPa and 25 MPa for compressive and flexural strength respectively. These results are of interest for the reuse of glass wool waste, QFS and similar waste streams in building ceramics.

Key words: Glass wool waste; Spodumene tailings; Recycling; Ceramics; Building application

1. Introduction

There are increasing concerns related to the depletion of some virgin natural resources and to the management of industrial side streams [1–5]. Examples of such side streams are glass wool waste and mine tailings. Glass wool waste is generated by construction and demolition activities and from glass wool industry, with annual production in Europe estimated to 800,000 tons [6,7]. Glass wool belongs to the family of mineral wools and is second in terms of volume, stone wool being the principal type of wool produced [7]. In comparison to stone wool, glass wool contents lesser CaO and Al_2O_3, but relatively higher amount of SiO_2 and Na_2O, the latter oxide reaching 16 wt.% in some cases [8]. Considering the European Commission notice on technical guidance on the classification of waste [9], glass wool wastes could be classified as waste glass-based fibrous materials (code 10 11 03) or insulation waste materials (code 17 06 04). Aside from glass wool wastes, mine tailings are generated at 5 to 7 billion tons yearly [10]. The valorisation of mine tailings is encouraged for the sustainability of the mining industry [1]. Amongst the possible valorisation options, ceramic processing aiming to produce building materials has been successfully explored in many tailings with adequate compositions [11–18]. For instance, Karhu et al., [13] studied the development of mullite based refractory ceramics from molybdenum, gold and quartz ore tailings, achieving best results with quartz ore tailings after adjustment of the Al/Si molar ratios with commercial boehmite. Fontes et al.,[19] reported the suitability of the finer fraction of iron rich tailings in the production of building ceramic tiles at 1200 °C. Tungsten tailings were found suitable as potential raw materials for commercial glasses [20]. Many other waste streams such as lignite fly ashes, bottom ash, waste coal, fly ashes, sewage sludge waste, municipal solid waste, tannery sludge, wine industry waste, dredged sediments, red mud, waste from borax mining and slags from various type of metal smelting were also reported as potential candidates for the development of waste based building ceramics [3,5,21–26]. However, the need of high sintering temperature is often a drawback in the manufacturing of building ceramics. High sintering temperature, mainly

above 1000 °C is problematic in terms of energy demand and production cost [3]. To reduce the sintering temperature, some commercial ingredients containing Na_2O, K_2O or MgO have been investigated as fluxing agents [27–30]. Due to its high content in alkali elements, some glass wastes have also been used as fluxing agent in clay brick production, favouring good mechanical properties at lower sintering temperature [3,31]. There are few reports on the reuse of stone wool wastes in ceramics [29,32]. However, reports on the reuse of glass wool wastes in ceramics are scarce, even though they are very close in terms of chemistry and mineralogy with some glass wastes successfully used as fluxing agents in ceramics, presenting an amorphous structure and 13-16 wt% Na_2O [3,8,31].

The present study deals with the utilization of spodumene tailings (quartz feldspars sand: QFS) and glass wool waste in the development of ceramics for potential application in construction. Here, glass wool waste was utilised as fluxing agent to lower the sintering temperatures and as a potential method towards its valorisation.

Several compositions were prepared with the as-received wool and ground glass wool. The prepared compositions were sintered at 750, 850 and 950 °C. These temperatures were chosen considering the melting behaviour of glass wool and the minimum temperature of 950 °C often used in the manufacturing of building fired bricks [22,33–35]. Scanning Electron Microscopy (SEM), thermogravimetric (TG/DSC) and X-ray diffraction (XRD) analyses were used to study the microstructure and phase evolution. Tests such as compressive and flexural strength, water absorption and apparent density were used to assess the possible suitability of the prepared ceramics for building applications.

2. Experimental

2.1. Materials

The QFS material was obtained from Keliber Oy, Finland. The glass wool used in this study was a by-product from the production of glass wool supplied by ISOVER Saint-Gobain, Finland. The

particle size distribution of the ground QFS and glass wool is presented in Figure 1. The QFS was milled in a ball mill of type Germatec TPR-D-950-V-FU-EH, Germany. Glass wool was ground in a compression and friction Mill of type Vibratory Disc Retsch (RS100): 1400 rpm; 1.5 min. Sodium silicate (modulus of 3.5 and 67 wt% of water) supplied by MERCK was used as deflocculating agent. The chemical composition and particle size information of ground glass wool and QFS are presented in Table 1 and Figure 1 respectively. Their mineralogy is presented in the subsection material characterisation in the results and discussion section.

Table 1. Chemical composition (wt%) of glass wool and QFS

Samples	SiO_2	Al_2O_3	Fe_2O_3	CaO	MgO	Na_2O	K_2O	TiO_2	P_2O_5	MnO	SO_3	Other	SUM
QFS	77.5	13.5	0.2	0.3	0.0	4.8	3.3	0.0	0.1	0.0	0	-	99.9
Glass wool	63.4	1.9	1	8.3	2.5	16.1	0.6	0.0	0.0	-	0.2	6	100

The 'other' value of 6% for glass wool in Table 1 stands for the loss of ignition (about 1.4 %) as well as unidentified compounds, mainly boron identified by ICP analysis in previous study [8].

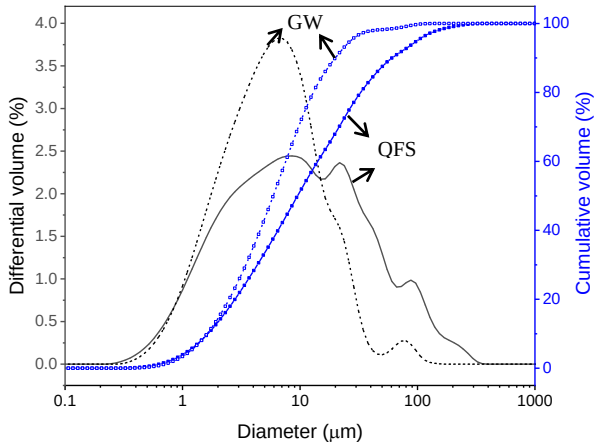

Figure 1: Particle size curves of ground QFS and glass wool (GW)

2.2. Specimens preparation

Specimens were prepared by dry mixing QFS with different amounts of glass wool. The dried QFS/glass wool powder was then added in a suitable amount of demineralised water containing

one-part weight of sodium silicate over 100 parts of dried QFS and mixed using an electric mixer at 1000 rpm, until obtention of a homogeneous plastic paste. The added sodium silicate acted as deflocculant agent, favouring the mixing and casting of the formulated pastes. The moulded (80×20×20 mm) formulations were dried in an oven at 60 °C for 24 hours, then unmoulded and further dried at 100 °C for 24 hours before being sintered at 750, 850 and 950 °C, heating rate of 5 °C per min and dwell time of 2 hours at each temperature.

The details on the mixture proportioning is presented in Table 2. Compositions 1 to 4 were prepared with the as-received wool, which only allowed easy addition of up to 10 g of glass wool per 100 g of QFS due to the fibrous nature of the wool. Compositions 5 to 8 were prepared with ground glass wool. Protective mask and gloves were used for handling glass wool to prevent possible concerns arising from glass wool inhalation.

Table 2: Mixture proportioning

Ref	QFS (g)	Glass wool (g)	Liquid sodium silicate (R=3.5) (g)	Water (g)	Sintering temperature
1 (Q100S1G0)	100	0	1	25	750,850, 950°C
2(Q100S1G2)	100	2	1	28	
3(Q100S1G6)	100	6	1	34	
4(Q100S1G10)	100	10	1	40	
5(Q100S1Gm 6)	100	6	1	16	
6(Q100S1Gm 10)	100	10	1	28	
7(Q100S1Gm 20)	100	20	1	31	
8(Q100S1Gm 40)	100	40	1	38	

2.3. Characterization methods

2.3.1. Compressive and flexural strength, water absorption and apparent density

The determination of the three-point flexural strength was performed using a Zwick testing machine with a maximum load of 100 kN and a loading rate of 0.05 kN/s. For each composition, three replicates specimens were tested. The supports span was 40 mm. The flexural strength (δ) was determined using the equation below:

$$\delta = 3FL/2bd^2$$

Where: δ is flexural strength in N/mm^2; F is maximum load in N; L is supports distance in mm; b is width of the tested beam in mm and d is height of the tested beam in mm.

The compressive strength was performed using the same Zwick testing machine, with a loading rate of 2.4 kN/s. For each composition, at least three replicates specimens were tested, and the average was regarded as the representative value of the strength. The error bars in Figures represent the standard deviation between measurements.

Water absorption was determined after samples immersion in deionized water for 24 hours and apparent density, using the Archimedes' principle according to SFS-EN 1936 standard.

2.3.2. XRD analyses

The starting materials and the prepared ceramics were ground to powder and examined by X-ray diffraction using a Rigaku Smartlab diffractometer, with a Cu K-beta radiation, step width of 0.02º, scan speed 4.0628 º/min, 2θ range of 5–80º, operated at 135 mA and 40 kV. The quantification of the crystalline phases was done using the Rietveld refinement method and 10 wt% rutile (TiO_2) as internal standard.

2.3.3. SEM/EDX analysis

The prepared ceramics were impregnated with low-viscosity epoxy resin. Samples were polished using diamond disc from 40 mm to 1 μm at a speed of 300-150 rpm. The samples were then coated with carbon and analysed using Scanning Electron Microscopy (SEM) and Energy Dispersive X-ray Spectroscopy (EDX) on a Zeiss Ultra Plus. Analyses were performed with both secondary and backscattered electron detectors, with 15 kV acceleration voltage and working distance of about 8.2 mm.

2.3.4. Thermogravimetry analysis

The Thermogravimetry analysis was performed with a simultaneous TG/DSC measurement in air, using a NETZSCH STA 449F3 TG/DSC instrument at a constant heating rate of 5 °C/min. The samples were heated from room temperature to 1000 °C.

3. Results and discussion

3.1. Materials characterization

The morphology of the as-received glass wool and ground glass wool is presented in Figure 2. The as-received glass wool presented a fibrous structure, with width of the fibre varying from about 1 to 4 μm while the length of unbroken fibres is above several hundred micrometres. It is observed from the SEM image of powdered wool that grinding was effective; the maximum length of residual fibres being about 10 μm. This agrees with previous studies on glass wool that suggested comminution methods based on compression and abrasion as effective for the destruction of the wools' fibrousness, which often constitutes a drawback for its reuse [7]. The EDS analysis of glass wool (not shown here) presented a homogenous composition of the fibres with about 47 wt% O, 33 wt% Si, 10.9 wt% Na, 6wt% Ca, 2 wt% Mg and 0.8 wt% Al, in agreement with data from XRF elemental composition in Table 1.

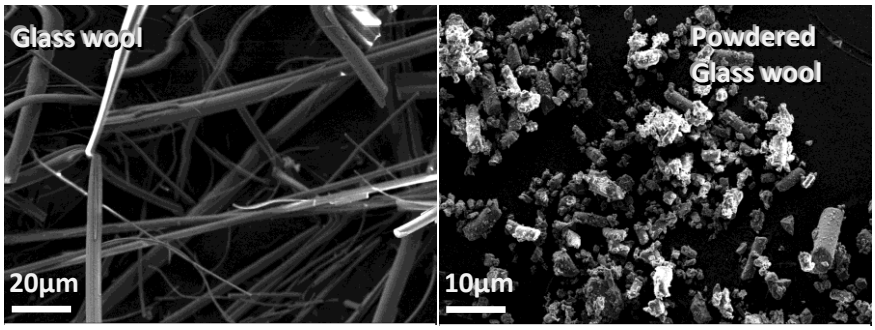

Figure 2: SEM images of as-received glass wool and powdered glass wool

The XRD patterns of QFS and glass wool are presented in Figure 3.

The glass wool was found to be completely amorphous, presenting no crystalline phases while QFS presented crystalline phase ascribed to quartz, SiO_2 (Pdf: 04-014-7568); albite,

$Na_{0.98}Ca_{0.02}Al_{1.02}Si_{2.98}O_8$ (Pdf: 04-017-1022); microcline, $KAlSi_3O_8$ (Pdf: 04-007-8600); and muscovite, $K_{0.8}Na_{0.2}Fe_{0.05}Al_{2.95}Si_{3.1}O_{10}(OH)_2$ (Pdf: 04-012-1906).

Previous studies showed that powdered QFS particles were made of single mineral phase corresponding to quartz, albite, and microcline identified in the XRD [30].

The amorphous structure of glass wool is consistent with previous studies on this material [8,36].

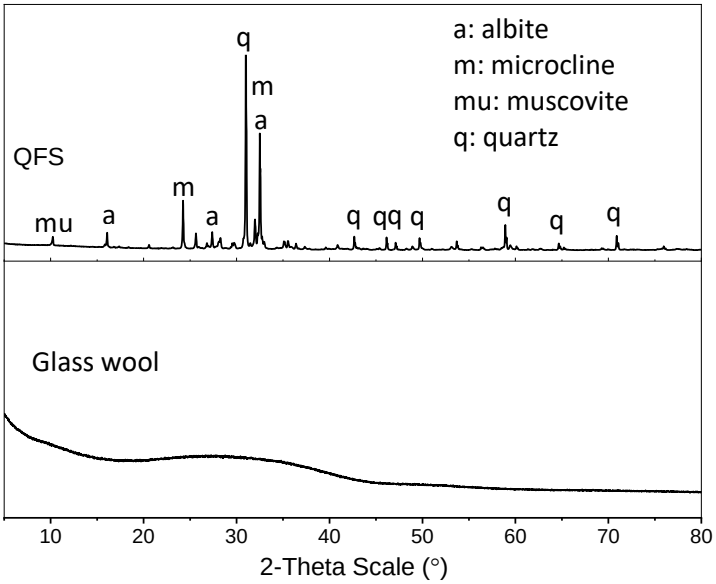

Figure 3: XRD patterns of QFS and glass wool

3.2. Phase composition of the prepared ceramics

Both temperature and glass wool content were observed to influence the composition of the formed ceramics. The compositions 1 (Q100S1G0), 6 (Q100S1Gm 10) and 8 (Q100S1Gm 40) thermally treated at 750 and 950 °C were selected for XRD analysis to better highlight this trend. Their XRD patterns are presented in Figure 4.

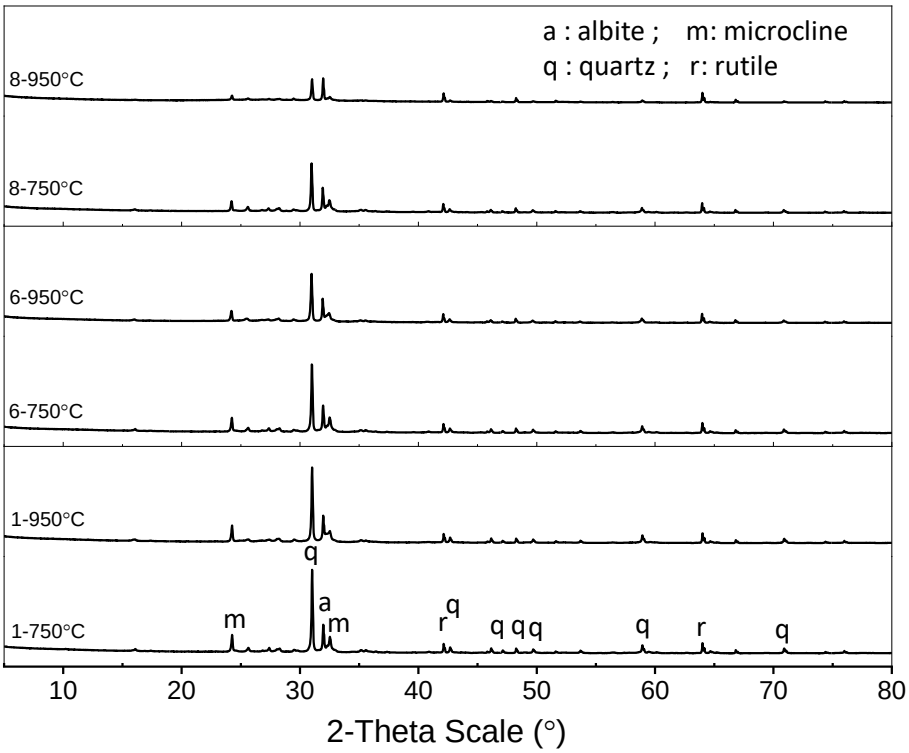

Figure 4: XRD patterns of compositions 1 (Q100S1G0), 6 (Q100S1Gm 10) and 8 (Q100S1Gm 40) prepared at indicated temperatures

It is observed that increasing the sintering temperature from 750 °C to 950 °C led to a reduction of the crystalline phases and was more marked as the percentage of glass wool increased in the mixture. This is ascribed to an increasing fluxing effect of glass wool as the temperature increased and the amorphous character of the glassy phase formed. This is well observed in the quantitative phase analysis presented in Figure 5.

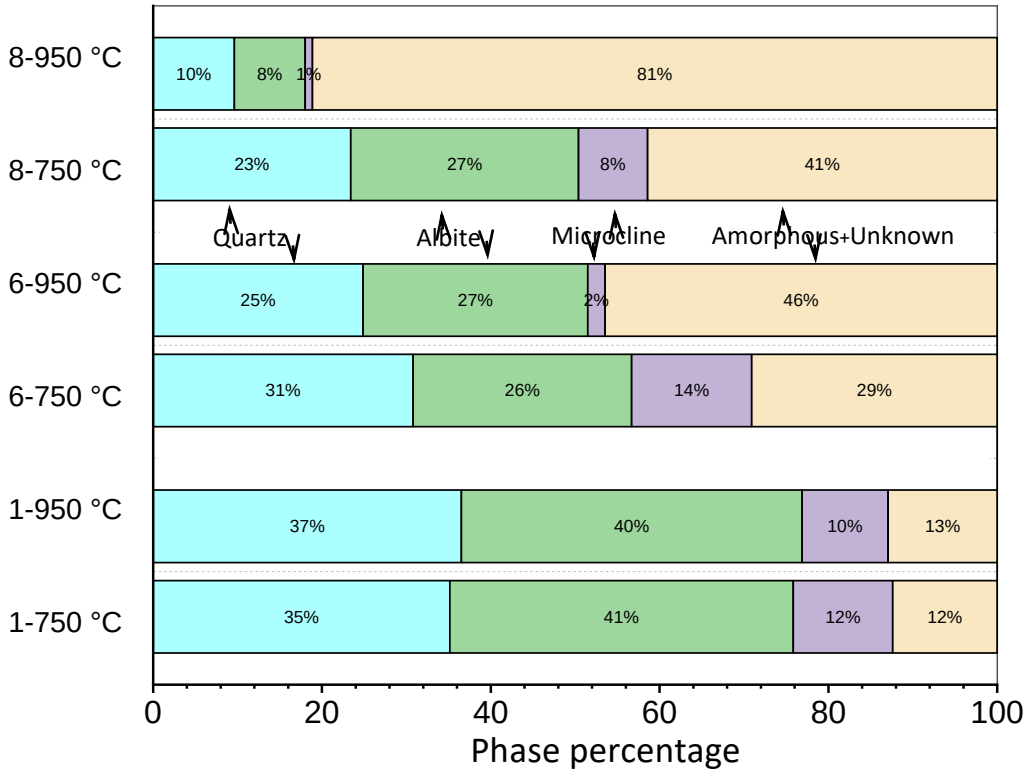

Figure 5: Quantitative phase analysis of compositions 1 (Q100S1G0), 6 (Q100S1Gm 10) and 8 (Q100S1Gm 40) prepared at indicated temperatures

In Figure 5, it is observed that only few changes occurred in the mineralogical composition of specimen 1 (Q100S1G0) when the temperature increased from 750 to 950 °C. Hence, QFS was relatively stable in this temperature range. However, specimens 6 and 8 containing glass wool were more sensitive to temperature compared to the control sample without glass wool. The amount of quartz and microcline were found to decrease with increasing temperature from 750 to 950 °C while the amount of amorphous phase increased. For instance, for composition 8, the proportion of quartz decreased from about 23% at 750 °C to 10% at 950 °C, while the amount of amorphous phase increased from about 41% at 750 °C to 81% at 950 °C. This result is in agreement with the decrease in intensity of crystalline reflections of quartz when the temperature increased from 750 to 950 °C (Figure 4), and consistent with previous studies on ceramic tiles containing soda-lime glass or boron-rich waste glass [37,38]. Similar observations have been also reported for waste based ceramics containing commercial Na_2O as fluxing agent [28,30]. For instance, in the study of fluxing

effect of Na_2O from sodium carbonate in the development of ceramic materials from coal bottom ash, it was observed that increasing Na_2O content in the samples induced a partial melting of crystals, resulting to an increase in the formation of amorphous liquid phase [28]. The amorphous nature of the formed glassy phase is also consistent with reported studies on foamed glass from mineral wool and glass waste containing about 20 wt% commercial borax ($Na_2B_4O_7 \cdot 10H_2O$) as fluxing agent; an amorphous glassy phase was observed within 800 -1000 °C before some crystalline phase of anorthite started to form [29]. Hence, the amount of Na_2O (16 wt%) in glass wool was enough for its potential use as fluxing agent in ceramic formulations. To further study the behaviour of the materials used and the formed ceramics, thermogravimetric analysis (TG/DSC) curves of QFS, glass wool and compositions 6 and 8 are presented in Figure 6.

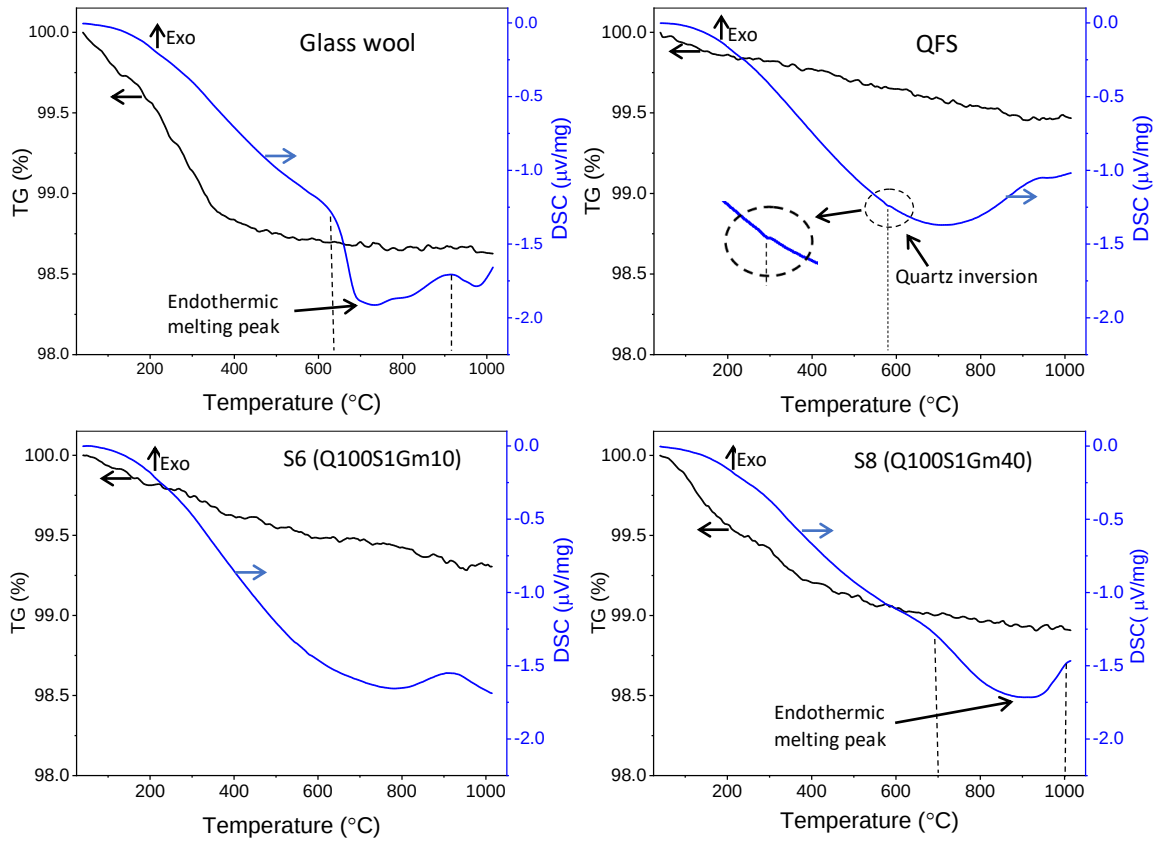

Figure 6: TG/DSC curves of glass wool, QFS and referred compositions

The mass loss at 1000 °C of glass wool and QFS was relatively low i.e., about 0.5% and 1.4% for QFS and glass wool respectively. It is observed that the major fraction of glass wool's mass loss is below 400 °C and is ascribed to the loss of possible adsorbed water or organic compound adsorbed during the manufacturing process. A broad endothermic peak starting around 600 °C up to 900 °C is ascribed to the melting of glass wool, which was confirmed by visual observation of the platinum crucible after the DSC experiment. The peak maximum intensity is around 700 °C suggesting this temperature as minimum for taking advantage of the fluxing effect of glass wool. The broad endothermic peak is slightly deconvoluted. The broadness and deconvolution are suggesting that all the constituents of glass wool are not melting at the same time, agreeing with the amorphous character observed in XRD, further indicating that glass wool would not melt at a certain melting point as pure solid crystalline phase, but would become gradually less viscous with the increase of the temperature. In this line, the small endothermic peak observed around 1000 °C is ascribed to possible solid-state reactions or melting of remaining specific constituent in glass wool. The DSC curve of QFS is not showing any endothermic melting peak. A small defection around 573 °C is ascribed to alpha-beta quartz inversion, which is consistent with mineral phases identified in the XRD analysis. The DSC curve of sample S6 (Q100S1Gm 10) presented no endothermic melting peak, while an endothermic melting peak was observed around 900 °C on the DSC curve of sample S8 (Q100S1Gm 40) and was confirmed by visual observation of the crucible after the experiment. Melting is known to rely on the chemical and mineralogical composition and is favored by increasing in alkali content and consequently lower the glass transition temperature [39,40].

Hence, due to its high content in Na_2O and the related effect on the Si/ (Ca+Na) ratio, glass wool was efficient in reducing the optimal sintering temperature of the formulated ceramics. Lower sintering temperature are of high interest in practical applications, as it leads to savings in energy demand and production costs.

3.3. Microstructural analysis

The microstructure of the prepared ceramic was found to be influenced by glass wool pretreatment, glass wool content and sintering temperature. Low magnification SEM images of referred specimens is presented is Figure 7.

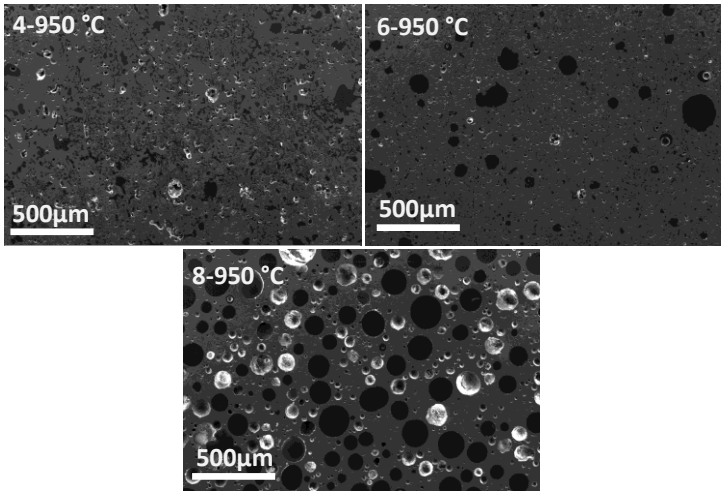

Figure 7: Secondary electron SEM images of compositions 4 (Q100S1G10), 6 (Q100S1Gm 10) and 8 (Q100S1Gm 40) sintered at 950 °C

It is observed that glass wool addition induced the formation of closed pores that was noticeable on the sample containing 40 parts of glass wool (i.e., Q100S1Gm 40). The SEM images present different features with closed pores more visualized on specimen 6 (Q100S1Gm10) and 8 (Q100S1Gm40) sintered at 950 °C. The black features observed on specimen 4 (Q100S1G10) sintered at 950 °C is ascribed to closed pores. The presence of closed pores in ceramic body containing glassy phase has been reported [37,38,41]. The possible origin of these closed pores was suggested to be entrapment of air in the relatively viscous melt and possible release of gas from specific raw materials [37]. For instance, the decomposition of the trace of muscovite present in QFS may have contributed to some gas release during viscous sintering. However, the most probable reason is the increase in the volume of the liquid phase with the increase of the sintering temperature, which promoted the melting of particles in the ceramic body and wrapped the voids between them, enclosing the gas that resulted to the formation of closed porosity [25,28].

It is noted that specimen 4 (Q100S1G10) presented more irregular pore in comparison to specimen 6 (Q100S1Gm10) where the pores tended to be more circular. Hence, it could be deduced that powdered wool has favored the production of a more regular microstructure with circular pores at 950 °C. The size of the pore increased with the increase of wool in the mixture with largest pores presenting a diameter of about 300 µm. These results are consistent with reported studies in foam ceramics were the pore size was observed to increase with increasing sintering temperature [42], as results of gas entrapment between particles by the liquid phase during the sintering process describer earlier [28]. The amount of formed liquid phase and consequently the ceramic properties also depend to the firing program [23] and high amount of closed porosity is often ascribed to overfiring [25].

Higher magnification SEM images of referred compositions at indicated temperatures are presented in Figure 8. Increasing the sintering temperature and wool content in the specimens affected the densification and microstructure. Specimen 1(Q100S1M0) made of QFS without wool addition presented a loose microstructure at 950 °C, with clear observation of the boundaries of QFS particles, and no sign of melting. This was at variance with specimens 4 (Q100S1G10), 6 (Q100S1Gm10) and 8 (Q100S1Gm 40) where the boundaries of residual starting material particles were not distinguished in the microstructure because of the formation of the melted phase. Elongated particles with light grey colour were ascribed to relic or new crystals from glass wool, due to their high content in calcium observed by EDS analysis.

The microstructure of these specimens presented a higher densification with increasing sintering temperature from 750 to 950 °C, as a result of the formation of more amorphous melted phase. These results are consistent to XRD analysis where a decrease of crystalline patterns were observed with the increase of the sintering temperature.

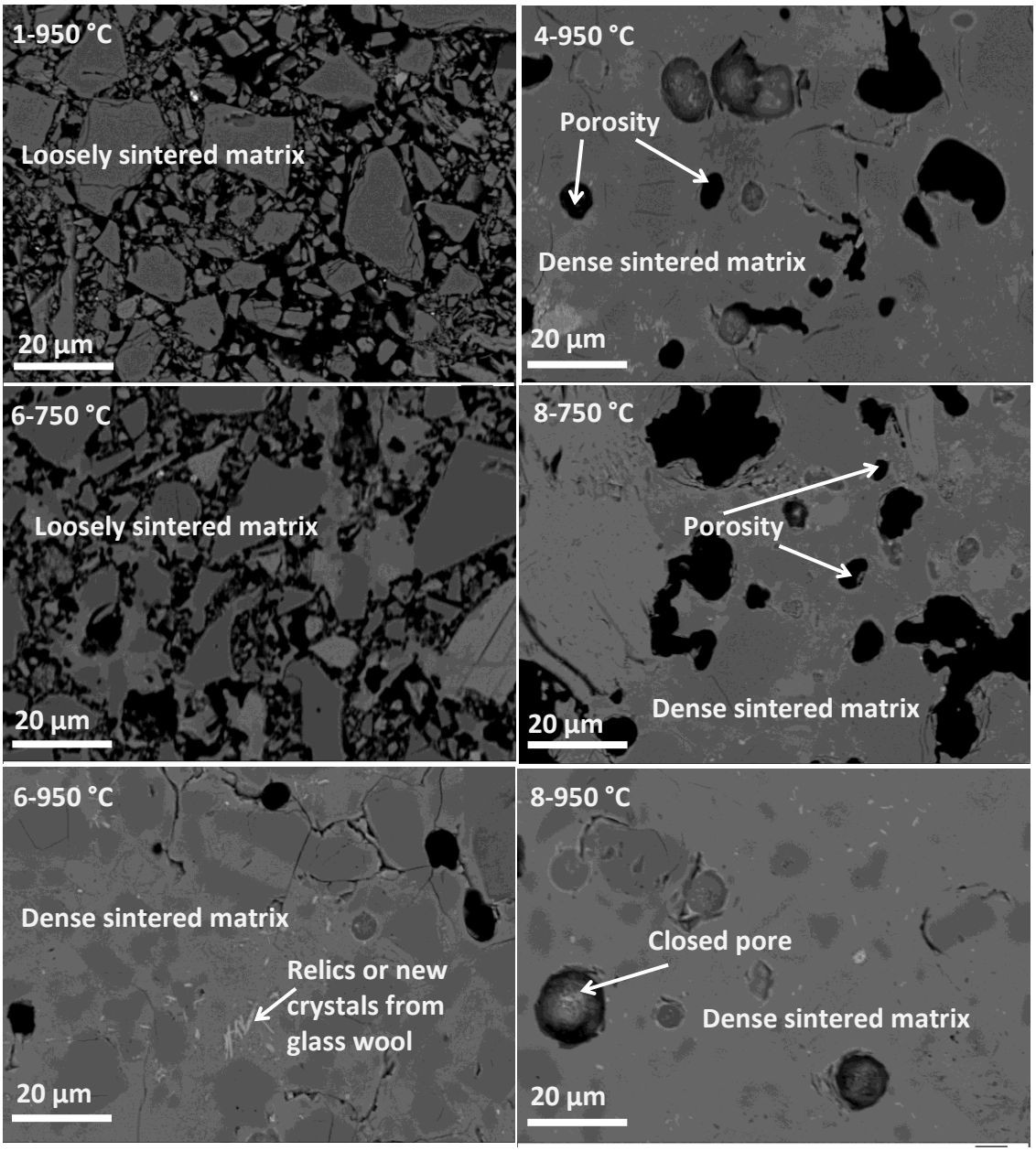

Figure 8: Back scattered SEM images of compositions 1(Q100S1M0), 4 (Q100S1G10), 6 (Q100S1Gm 10) and 8 (Q100S1Gm 40) prepared at indicated temperatures

The evolution of the composition of the glassy phase of specimen 8 (Q100S1Gm 40) performed by EDS analysis on 132 points at 750 and 950 °C is presented in Figure 9.

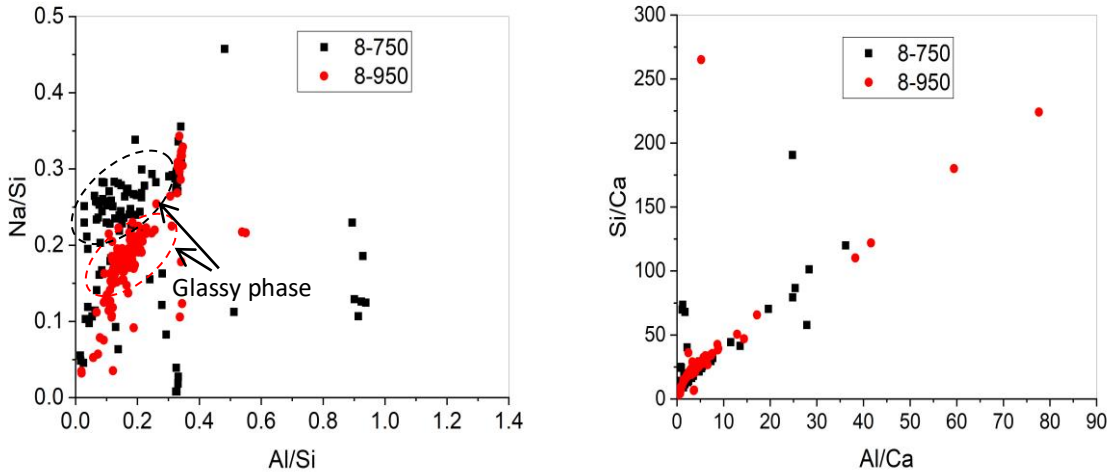

Figure 9: Composition of points analyzed by EDS on specimen 8 (Q100S1Gm 40) sintered at 750 and 950 °C.

From Figure 9, it is observed that increasing the sintering temperature from 750 to 950 °C has led to a change of the composition of the melting phase, with a more uniform composition marked by less scattered points at 950 °C. The area of high concentration of points (circled with dashed line) corresponds to the glassy phase while isolated points correspond to the relic of the starting materials. It is also noted that the Na/Si atomic ratio of the glassy phase is decreasing with the increase of the sintering temperature. This is ascribed to an increase in the dissolution rate of quartz and other QFS minerals with the increase of the sintering temperature, in agreement with the results obtained in XRD analysis. It is seen that the Al/Ca atomic ratio in the glassy phase varied between 0 and 10, being around 5 for most points, agreeing with the composition of glass wool and QFS. These results are consistent with reported studies on glass formation from aluminosilicates where formation of viscous liquid, depending on the composition and particle size of starting materials, was observed to be favoured by an increase of the sintering temperature [14,39,43]. In this line, the higher content of glass wool in specimen 8 (Q100S1Gm 40) reduced the proportion of silica known to decrease the dissolution rate in multicomponent aluminosilicate glasses. Hence, the formation of

glassy phase from the relatively low temperature of 750 °C is ascribed to the increase in the proportion of network modifiers such as CaO and mainly Na_2O which function as fluxing agents.

Conventional building ceramics such as clay bricks and roofing tile are often sintered at 950–1200 °C [19,22,44–46]. Thus, the production of building ceramics incorporating glass wool as fluxing agent is expected to be more cost efficient, considering the reduced sintering temperature induced by the fluxing effect of glass wool.

3.4. Properties of ceramics prepared with the as-received glass wool

The water absorption and compressive strength of building materials are amongst the main properties to be considered when the building materials are planned to be subjected to severe weathering environment [47].

As for the case for microstructural analysis, the physical properties of the prepared ceramics were observed to be influenced by glass wool content and sintering temperature. The properties (compressive and flexural strength, water absorption and apparent density) of the ceramic prepared with the as-received glass wool are presented in Figure 10.

The compressive strength of specimens prepared with the as-received glass wool varied from about 0 to 35 MPa depending on the wool addition and sintering temperature. Highest strength was achieved at 950 °C with specimens 4(Q100S1G10), containing 10 parts of as-received glass wool. Hence, both wool addition and sintering temperature were favorable to strength development. It is noted that the compressive strength of specimens prepared with the addition of 6 parts of glass wool was above 20 MPa when sintered at 950 °C, while the compressive strength of specimens prepared with 2 parts or no wool addition was below 10 MPa. This indicates the positive effect of the as-received glass wool on the development of mechanical properties.

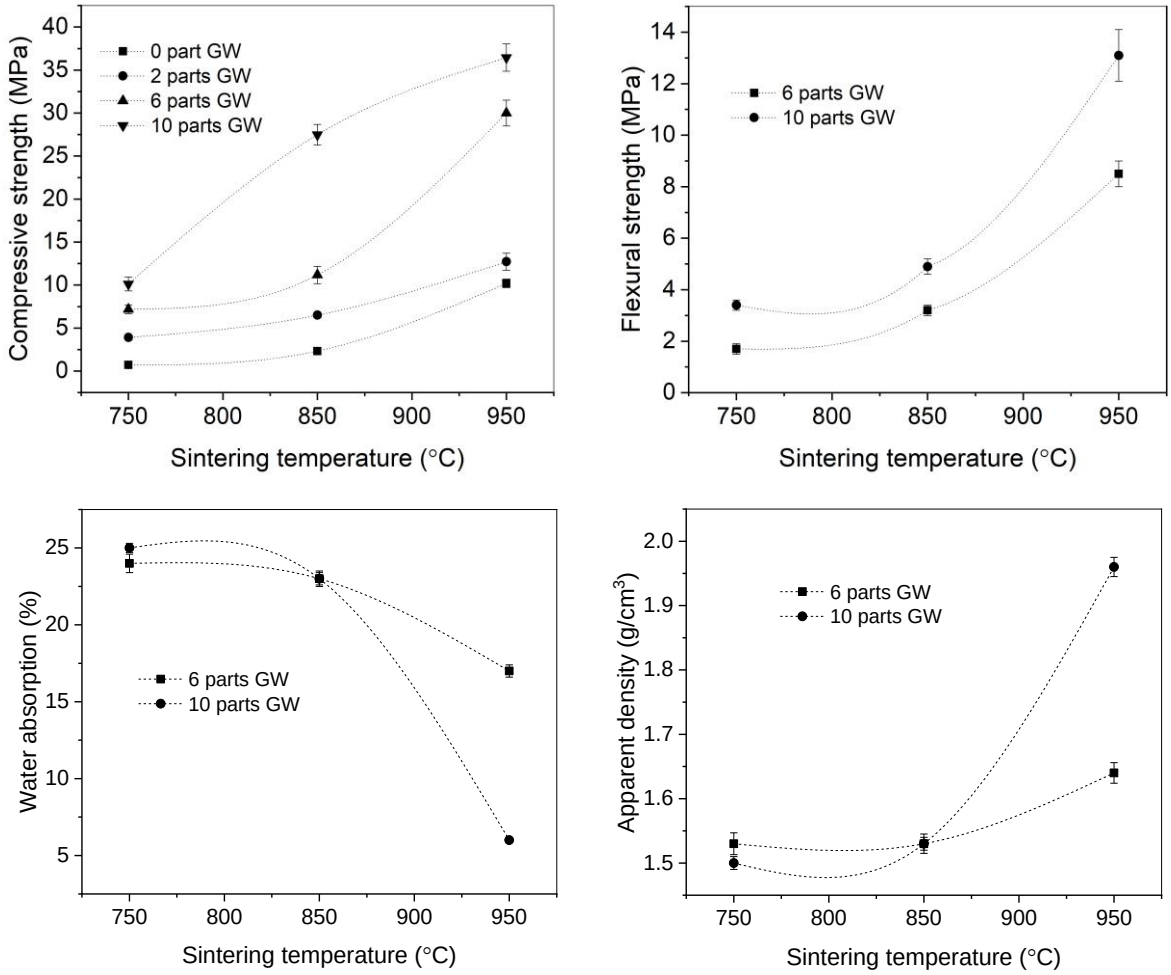

Figure 10: Properties of ceramics prepared with 0 to 10 parts of as-received glass wool (GW) per 100 parts of QFS

Due to the poor performances in compression of specimens 1(Q100S1G0) and 2(Q100S1G2) in Table 2, they were not considered for other properties (flexural strength, apparent density and water absorption). The maximum flexural strength was about 10 MPa for specimen 4(Q100S1G10) after sintering at 950 °C. Water absorption ranged from about 8 to 25 % while apparent density ranged from about 1.5 to 1.9 g/cm^3. A reduction of water absorption is observed with an increase of the proportion of glass wool and sintering temperature, at variance to density.

3.5. Properties of ceramics prepared with the ground glass wool

The properties (compressive and flexural strength, water absorption and apparent density) of the ceramics prepared with the ground glass wool is presented in Figure 11.

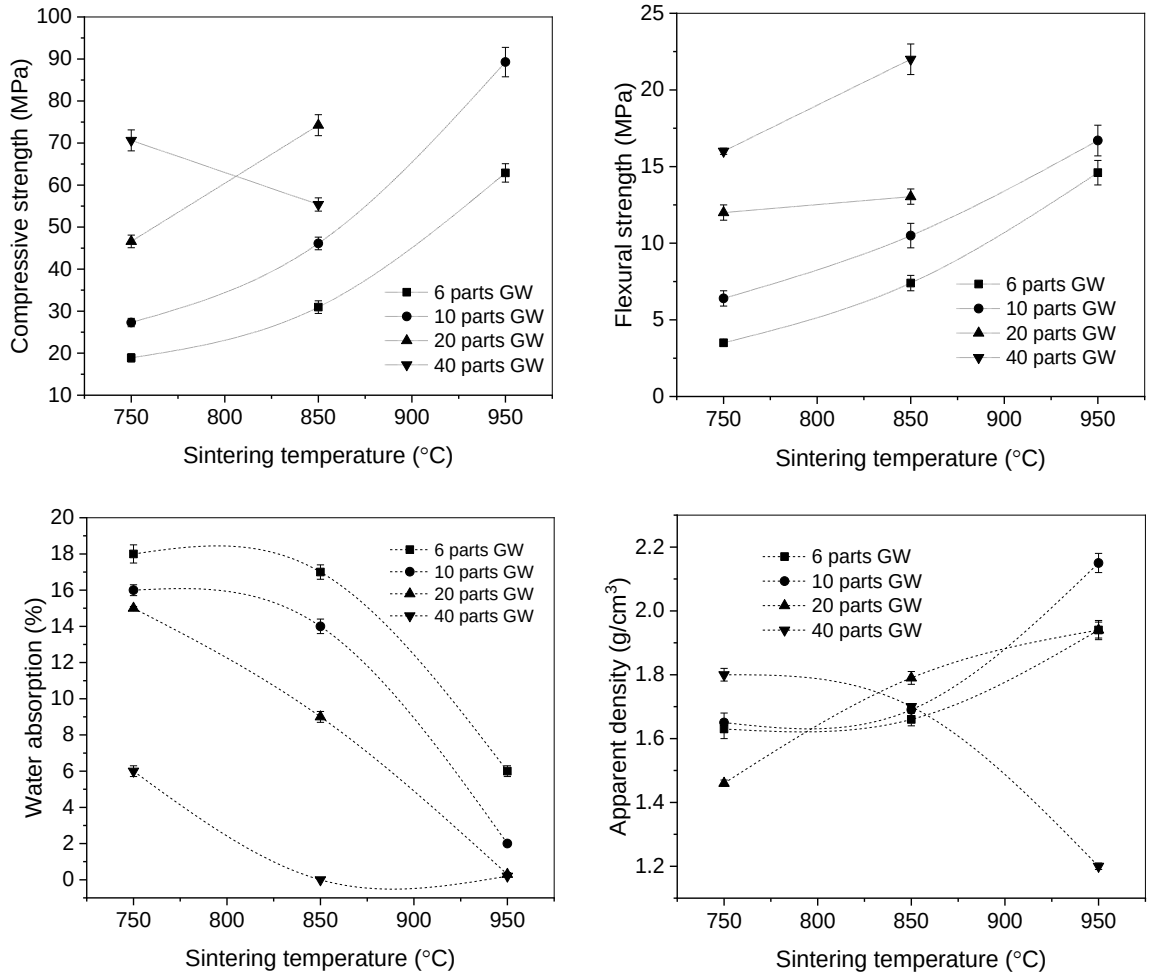

Figure 11: Properties of ceramics prepared with 6 to 40 parts of ground glass wool (GW) per 100 parts of QFS

Specimens 7 (Q100S1Gm 20) and 8 (Q100S1Gm 40) deformed at 950 °C and no compressive strength nor flexural strength were tested at this temperature. The compressive strength of specimens prepared with 6 to 40 parts glass wool varied from about 20 to 90 MPa depending on glass wool addition and sintering temperature. The flexural strength of 5–25 MPa was achieved with these formulations. The highest compressive strength was achieved at 950 °C with specimen

6(Q100S1Gm 10). In most cases, both compressive and flexural strength presented a trend of increase with the increase of sintering temperature and glass wool in the mixture, except for the specimen containing 40 parts of glass wool where the compressive strength was found to reduce when the temperature raised from 750 to 850 °C. The reason for reduction is attributed to the formation of closed pores while a different trend is observed in flexural strength because of better glassy phase formation which induced higher bonding strength with increasing the sintering temperature. Specimen prepared with 6 parts glass wool presented a compressive strength of about 20, 30 and 60 MPa at 750, 850 and 950 °C, respectively. In contrast, at the same sintering temperature, specimen prepared with 10 parts glass wool presented a compressive strength of about 30, 50 and 90 MPa, respectively. This clearly show the effect of both glass wool and temperature on the sintering and final properties.

The compressive strength values of all the specimens prepared with ground glass wool were above 20 MPa, the minimum requirement of compressive strength for building bricks prescribed in ASTM C62 standard for building bricks [47]. Hence, the prepared ceramics can be potentially used in structural applications. Furthermore, the values of compressive strength of the compositions made of 40 parts of glass wool over 100 parts of QFS was about 80 MPa at the lowest sintering temperature of 750 °C, almost like that of specimen containing moderated amount (10 parts) of wool sintered at 950 °C.

Besides, it is important to note that the mechanical properties of compositions containing ground glass wool were superior to their counterpart containing the same percentage of the as-received wool. This suggest that milling the wool was beneficial for strength development. Additionally, it was difficult to add more than 10 wt% parts of non-milled glass wool over 100 parts of QFS because of its high specific volume. Hence, grinding the wool offers additional advantage for designing options, with possibility to prepare ceramic mixtures containing any proportion of glass

wool. These results are comparable to those obtained with the use of waste glasses as fluxing agent in the preparation of building ceramics [3,31].

The compressive strength values of the ceramics from ground wool in this study are superior to that of reported values of many waste-based and natural-based building ceramics [48–51] sintered at higher temperatures (800–1100 °C). Considering the negative impact of high sintering temperature on the production cost, the prepared ceramics are expected to present a lower processing cost. Hence, the development of building ceramics containing large proportion of glass wool can contribute in reducing the sintering temperature and the production cost, with additional advantage on waste management through the upcycling of glass wool waste. The results obtained here can thus constitute a baseline for further investigations for a wider use of glass wool as fluxing agent for waste and even clay-based building ceramics. For the case of building ceramics fully made of industrial side streams as the case in this study, their use can contribute in both waste management and saving of virgin resources used as feedstock materials for the ceramic or building industry.

Water absorption values ranged from about 0 to 16%. A reduction of water absorption was observed with an increase of glass wool and sintering temperature. The specimen prepared with 10 parts glass wool presented a water absorption of 16, 14 and 2% at 750, 850 and 950 °C, respectively, while the water absorption of the specimen prepared with 40 parts glass wool was about 0% at 850 and 950 °C. This confirms again the effect of glass wool addition as fluxing agent on the ceramic properties. According to ASTM C62 standard on building bricks, the values of water absorption should be below 17 % for building brick that will be subjected to severe weathering environments [47]. Hence, based on water absorption values, specimens prepared with at least 10 parts of glass wool over 100 parts of QFS could be suitable formulations for building bricks for severe weathering environments. The apparent density of most of the specimens increased with the sintering temperature, from about 1.4–1.8 g/cm^3 at 750 °C to about 1.5–2.1 g/cm^3 at 950 °C. However, the

apparent density of specimen made of 40 parts glass wool decreased with increasing sintering temperature, mainly between 850 and 950 °C, achieving a value of 1.2 g/cm^3 at 950 °C. The reason for that is the formation of closed pores observed in the SEM analysis. Hence, it could be deduced that higher proportion of wool induced the formation of closed pores when the temperature increased.

Images of referred specimens treated at indicated temperature are presented in Figure 12. The deformation of specimen 8 (Q100S1Gm40) at 950 °C is observed, due to excess formation of the glassy phase. However, this characteristic could also be used to prepare decorative materials, as shown by aesthetic appearance of circular specimens prepared with this formulation. Hence a synergetic use of QFS and glass wool in the production of ceramic materials could be of interest for the development of both building and decorative ceramics.

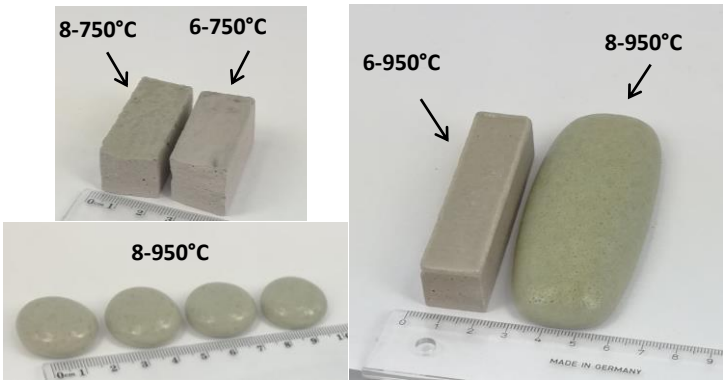

Figure 12: Photo of specimens from compositions 6 (Q100S1Gm 10) and 8 (Q100S1Gm 40) prepared at indicated temperatures

3.6. Conclusions

This study investigated the utilisation of glass wool waste and lithium mine tailings from spodumene ore (QFS) in the development of building ceramics. The QFS mainly consisted of

quartz, albite and microcline while the glass wool was amorphous, mainly consisting of SiO_2 (63%), Na_2O (16%) and CaO (8%). The prepared compositions were sintered at 750, 850 and 950 °C. The results showed that glass wool acted as fluxing agent, with fluxing effects comparable to that of some commercial fluxing agents and melting reactions evidenced from about 700 °C. Grinding glass wool improved its reactivity, enhancing densification and strength development at lower temperatures. The effect of glass wool was observed to be significant from about 10 wt%. However, increasing wool content to about 40wt% favoured the development of good mechanical properties at 750 °C, reducing the energy associated to the sintering. The properties of the prepared building ceramics satisfied the requirement of building materials according to ASTM C62, achieving high performance values of 90 MPa and 25 MPa for compressive and flexural strength respectively. The water absorption values ranged from 0 to 25%; the values decreased with increasing sintering temperature and glass wool content. Apparent density of the samples varied from about 1.5 to 2.1 g/cm^3. These results are of interest for the reuse of waste glass wool, QFS and similar waste streams in building ceramics.

Acknowledgements

This work was performed under the framework of the "GEOBOT" project, supported by the European Regional Development Fund (ERDF), Pohjois-Pohjanmaa Council of Oulu Region and Vipuvoimaa EU:lta 2014-2020 and companies Boliden Harjavalta Oy, Keliber Oy and Saint-Gobain Finland Oy. Part of the work was carried out with the support of the Centre for Material Analysis, University of Oulu, Finland. The contribution of Merja Peratalo in laboratory work is also appreciated.

References

[1] P.H.-M. Kinnunen, A.H. Kaksonen, Towards circular economy in mining: Opportunities and bottlenecks for tailings valorization, Journal of Cleaner Production. 228 (2019) 153–160. https://doi.org/10.1016/j.jclepro.2019.04.171.

[2] Y. Zhang, Y. Hu, N. Sun, R. Liu, Z. Wang, L. Wang, W. Sun, Systematic review of feldspar beneficiation and its comprehensive application, Minerals Engineering. 128 (2018) 141–152. https://doi.org/10.1016/j.mineng.2018.08.043.

[3] V. Karayannis, A. Moutsatsou, A. Domopoulou, E. Katsika, C. Drossou, A. Baklavaridis, Fired ceramics 100% from lignite fly ash and waste glass cullet mixtures, Journal of Building Engineering. 14 (2017) 1–6. https://doi.org/10.1016/j.jobe.2017.09.006.

[4] P. Sormunen, T. Kärki, Recycled construction and demolition waste as a possible source of materials for composite manufacturing, Journal of Building Engineering. 24 (2019) 100742. https://doi.org/10.1016/j.jobe.2019.100742.

[5] A. Al-Fakih, B.S. Mohammed, M.S. Liew, E. Nikbakht, Incorporation of waste materials in the manufacture of masonry bricks: An update review, Journal of Building Engineering. 21 (2019) 37–54. https://doi.org/10.1016/j.jobe.2018.09.023.

[6] O. Väntsi, T. Kärki, Mineral wool waste in Europe: a review of mineral wool waste quantity, quality, and current recycling methods, Journal of Material Cycles and Waste Management. 16 (2014) 62–72. https://doi.org/10.1007/s10163-013-0170-5.

[7] J. Yliniemi, O. Laitinen, P. Kinnunen, M. Illikainen, Pulverization of fibrous mineral wool waste, Journal of Material Cycles and Waste Management. 20 (2018) 1248–1256.

[8] J. Yliniemi, P. Kinnunen, P. Karinkanta, M. Illikainen, Utilization of Mineral Wools as Alkali-Activated Material Precursor, Materials (Basel). 9 (2016). https://doi.org/10.3390/ma9050312.

[9] EUROPEAN COMMISSION, Commission notice on technical guidance on the classification of waste, (2018).

[10] P. Kinnunen, A. Ismailov, S. Solismaa, H. Sreenivasan, M.-L. Räisänen, E. Levänen, M. Illikainen, Recycling mine tailings in chemically bonded ceramics – A review, Journal of Cleaner Production. 174 (2018) 634–649. https://doi.org/10.1016/j.jclepro.2017.10.280.

[11] N.V. Boltakova, G.R. Faseeva, R.R. Kabirov, R.M. Nafikov, Yu.A. Zakharov, Utilization of inorganic industrial wastes in producing construction ceramics. Review of Russian experience for the years 2000–2015, Waste Management. 60 (2017) 230–246. https://doi.org/10.1016/j.wasman.2016.11.008.

[12] Y. Chen, Y. Zhang, T. Chen, Y. Zhao, S. Bao, Preparation of eco-friendly construction bricks from hematite tailings, Construction and Building Materials. 25 (2011) 2107–2111. https://doi.org/10.1016/j.conbuildmat.2010.11.025.

[13] M. Karhu, J. Lagerbom, S. Solismaa, M. Honkanen, A. Ismailov, M.-L. Räisänen, E. Huttunen-Saarivirta, E. Levänen, P. Kivikytö-Reponen, Mining tailings as raw materials for reaction-sintered aluminosilicate ceramics: Effect of mineralogical composition on microstructure and properties, Ceramics International. (2018). https://doi.org/10.1016/j.ceramint.2018.11.180.

[14] P.N. Lemougna, J. Yliniemi, A. Ismailov, E. Levanen, P. Tanskanen, P. Kinnunen, J. Roning, M. Illikainen, Spodumene tailings for porcelain and structural materials: Effect of temperature (1050–1200 °C) on the sintering and properties, Minerals Engineering. (2019) 105843. https://doi.org/10.1016/j.mineng.2019.105843.

[15] R. Li, Y. Zhou, C. Li, S. Li, Z. Huang, Recycling of industrial waste iron tailings in porous bricks with low thermal conductivity, Construction and Building Materials. 213 (2019) 43–50. https://doi.org/10.1016/j.conbuildmat.2019.04.040.

[16] A.L. Murmu, A. Patel, Towards sustainable bricks production: An overview, Construction and Building Materials. 165 (2018) 112–125. https://doi.org/10.1016/j.conbuildmat.2018.01.038.
[17] S. Solismaa, A. Ismailov, M. Karhu, H. Sreenivasan, M. Lehtonen, P. Kinnunen, M. Illikainen, M.L. Räisänen, Valorization of Finnish mining tailings for use in the ceramics industry, Bulletin of the Geological Society of Finland. Vol. 90, (2018) 33-54.
[18] Y. Taha, M. Benzaazoua, R. Hakkou, M. Mansori, Coal mine wastes recycling for coal recovery and eco-friendly bricks production, Minerals Engineering. 107 (2017) 123–138. https://doi.org/10.1016/j.mineng.2016.09.001.
[19] W.C. Fontes, J.M. Franco de Carvalho, L.C.R. Andrade, A.M. Segadães, R.A.F. Peixoto, Assessment of the use potential of iron ore tailings in the manufacture of ceramic tiles: From tailings-dams to "brown porcelain," Construction and Building Materials. 206 (2019) 111–121. https://doi.org/10.1016/j.conbuildmat.2019.02.052.
[20] P. Alfonso, O. Tomasa, M. Garcia-Valles, M. Tarragó, S. Martínez, H. Esteves, Potential of tungsten tailings as glass raw materials, Materials Letters. 228 (2018) 456–458. https://doi.org/10.1016/j.matlet.2018.06.098.
[21] H. Slimanou, D. Eliche-Quesada, S. Kherbache, N. Bouzidi, A. /K. Tahakourt, Harbor Dredged Sediment as raw material in fired clay brick production: Characterization and properties, Journal of Building Engineering. 28 (2020) 101085. https://doi.org/10.1016/j.jobe.2019.101085.
[22] R. Taurino, D. Ferretti, L. Cattani, F. Bozzoli, F. Bondioli, Lightweight clay bricks manufactured by using locally available wine industry waste, Journal of Building Engineering. 26 (2019) 100892. https://doi.org/10.1016/j.jobe.2019.100892.
[23] W.E. Lee, A.R. Boccaccini, J.A. Labrincha, C. Leonelli, C.H. Drummond III, C.R. Cheeseman, Ceramic Technology and Sustainable Development. (cover story), American Ceramic Society Bulletin. 86 (2007) 18–25.
[24] M. Dondi, G. Guarini, M. Raimondo, C. Zanelli, D.D. Fabbriche, A. Agostini, Recycling the insoluble residue from titania slag dissolution (tionite) in clay bricks, Ceramics International. 36 (2010) 2461–2467. https://doi.org/10.1016/j.ceramint.2010.08.007.
[25] L.M. Schabbach, F. Andreola, L. Barbieri, I. Lancellotti, E. Karamanova, B. Ranguelov, A. Karamanov, Post-treated incinerator bottom ash as alternative raw material for ceramic manufacturing, Journal of the European Ceramic Society. 32 (2012) 2843–2852. https://doi.org/10.1016/j.jeurceramsoc.2012.01.020.
[26] N. Quijorna, M. de Pedro, M. Romero, A. Andrés, Characterisation of the sintering behaviour of Waelz slag from electric arc furnace (EAF) dust recycling for use in the clay ceramics industry, Journal of Environmental Management. 132 (2014) 278–286. https://doi.org/10.1016/j.jenvman.2013.11.012.
[27] G.R. dos Santos, A.R. Salvetti, M.D. Cabrelon, M.R. Morelli, Synthetic flux as a whitening agent for ceramic tiles, Journal of Alloys and Compounds. 615 (2014) S459–S461. https://doi.org/10.1016/j.jallcom.2013.12.001.
[28] X. Ge, M. Zhou, H. Wang, L. Chen, X. Li, X. Chen, Effects of flux components on the properties and pore structure of ceramic foams produced from coal bottom ash, Ceramics International. 45 (2019) 12528–12534. https://doi.org/10.1016/j.ceramint.2019.03.190.
[29] R. Ji, Y. Zheng, Z. Zou, Z. Chen, S. Wei, X. Jin, M. Zhang, Utilization of mineral wool waste and waste glass for synthesis of foam glass at low temperature, Construction and Building Materials. 215 (2019) 623–632. https://doi.org/10.1016/j.conbuildmat.2019.04.226.
[30] P.N. Lemougna, J. Yliniemi, A. Ismailov, E. Levanen, P. Tanskanen, P. Kinnunen, J. Roning, M. Illikainen, Recycling lithium mine tailings in the production of low temperature (700–900 °C) ceramics: Effect of ladle slag and sodium compounds on the processing and final properties, Construction and Building Materials. 221 (2019) 332–344. https://doi.org/10.1016/j.conbuildmat.2019.06.078.

[31] N. Phonphuak, S. Kanyakam, P. Chindaprasirt, Utilization of waste glass to enhance physical–mechanical properties of fired clay brick, Journal of Cleaner Production. 112 (2016) 3057–3062. https://doi.org/10.1016/j.jclepro.2015.10.084.
[32] Z. Chen, H. Wang, R. Ji, L. Liu, C. Cheeseman, X. Wang, Reuse of mineral wool waste and recycled glass in ceramic foams, Ceramics International. 45 (2019) 15057–15064. https://doi.org/10.1016/j.ceramint.2019.04.242.
[33] M. Sutcu, E. Erdogmus, O. Gencel, A. Gholampour, E. Atan, T. Ozbakkaloglu, Recycling of bottom ash and fly ash wastes in eco-friendly clay brick production, Journal of Cleaner Production. 233 (2019) 753–764. https://doi.org/10.1016/j.jclepro.2019.06.017.
[34] J. Rukijkanpanich, N. Thongchai, Burned brick production from residues of quarrying process in Thailand, Journal of Building Engineering. 25 (2019) 100811. https://doi.org/10.1016/j.jobe.2019.100811.
[35] A. Nzeukou, V. Kamgang, U. Melo, A. Njoya, P. Lemougna, N. Fagel, Industrial Potentiality of Alluvial Clays Deposits from Cameroon: Influence of Lateritic Clayey Admixture for Fired Bricks Production, Journal of Minerals and Materials Characterization and Engineering. 1 (2013) 236–244. https://doi.org/10.4236/jmmce.2013.15037.
[36] K. do Carmo e Silva Defáveri, L.F. dos Santos, J.M. Franco de Carvalho, R.A.F. Peixoto, G.J. Brigolini, Iron ore tailing-based geopolymer containing glass wool residue: A study of mechanical and microstructural properties, Construction and Building Materials. 220 (2019) 375–385. https://doi.org/10.1016/j.conbuildmat.2019.05.181.
[37] M. Lassinantti Gualtieri, C. Mugoni, S. Guandalini, A. Cattini, D. Mazzini, C. Alboni, C. Siligardi, Glass recycling in the production of low-temperature stoneware tiles, Journal of Cleaner Production. 197 (2018) 1531–1539. https://doi.org/10.1016/j.jclepro.2018.06.264.
[38] F. Matteucci, M. Dondi, G. Guarini, Effect of soda-lime glass on sintering and technological properties of porcelain stoneware tiles, Ceramics International. 28 (2002) 873–880. https://doi.org/10.1016/S0272-8842(02)00067-6.
[39] V. Schultz-Falk, K. Agersted, P.A. Jensen, M. Solvang, Melting behaviour of raw materials and recycled stone wool waste, Journal of Non-Crystalline Solids. 485 (2018) 34–41. https://doi.org/10.1016/j.jnoncrysol.2018.01.035.
[40] M.M. Smedskjaer, M. Solvang, Y. Yue, Crystallisation behaviour and high-temperature stability of stone wool fibres, Journal of the European Ceramic Society. 30 (2010) 1287–1295.
[41] A.P. Luz, S. Ribeiro, Use of glass waste as a raw material in porcelain stoneware tile mixtures, Ceramics International. 33 (2007) 761–765. https://doi.org/10.1016/j.ceramint.2006.01.001.
[42] T. Liu, C. Lin, J. Liu, L. Han, H. Gui, C. Li, X. Zhou, H. Tang, Q. Yang, A. Lu, Phase evolution, pore morphology and microstructure of glass ceramic foams derived from tailings wastes, Ceramics International. 44 (2018) 14393–14400. https://doi.org/10.1016/j.ceramint.2018.05.049.
[43] P. Kinnunen, H. Sreenivasan, C.R. Cheeseman, M. Illikainen, Phase separation in alumina-rich glasses to increase glass reactivity for low-CO2 alkali-activated cements, Journal of Cleaner Production. 213 (2019) 126–133. https://doi.org/10.1016/j.jclepro.2018.12.123.
[44] N. Phonphuak, C. Saengthong, A. Srisuwan, Physical and mechanical properties of fired clay bricks with rice husk waste addition as construction materials, Materials Today: Proceedings. 17 (2019) 1668–1674. https://doi.org/10.1016/j.matpr.2019.06.197.
[45] X. Xu, J. Song, Y. Li, J. Wu, X. Liu, C. Zhang, The microstructure and properties of ceramic tiles from solid wastes of Bayer red muds, Construction and Building Materials. 212 (2019) 266–274. https://doi.org/10.1016/j.conbuildmat.2019.03.280.
[46] A.W. Bruno, D. Gallipoli, C. Perlot, H. Kallel, Thermal performance of fired and unfired earth bricks walls, Journal of Building Engineering. 28 (2020) 101017. https://doi.org/10.1016/j.jobe.2019.101017.

[47] ASTM C62, ASTM C62-99: Standard Specification for Building Brick (Solid Masonry Units Made From Clay or Shale), (1999).
[48] D. Eliche-Quesada, J. Leite-Costa, Use of bottom ash from olive pomace combustion in the production of eco-friendly fired clay bricks, Waste Management. 48 (2016) 323–333. https://doi.org/10.1016/j.wasman.2015.11.042.
[49] O. Kizinievič, V. Kizinievič, I. Pundiene, D. Molotokas, Eco-friendly fired clay brick manufactured with agricultural solid waste, Archives of Civil and Mechanical Engineering. 18 (2018) 1156–1165. https://doi.org/10.1016/j.acme.2018.03.003.
[50] C. Leiva, C. Arenas, B. Alonso-fariñas, L.F. Vilches, B. Peceño, M. Rodriguez-galán, F. Baena, Characteristics of fired bricks with co-combustion fly ashes, Journal of Building Engineering. 5 (2016) 114–118. https://doi.org/10.1016/j.jobe.2015.12.001.
[51] J.P. Temga, J.R. Mache, A.B. Madi, J.P. Nguetnkam, D.L. Bitom, Ceramics applications of clay in Lake Chad Basin, Central Africa, Applied Clay Science. 171 (2019) 118–132. https://doi.org/10.1016/j.clay.2019.02.003.